



HAL
open science

High-fat Feeding Promotes Obesity via Insulin Receptor/PI3k-Dependent Inhibition of SF-1 VMH Neurons

Tim Klöckener, Simon Hess, Bengt F. Belgardt, Lars Paeger, Linda A. Verhagen, Andreas Husch, Jong-Woo Sohn, Brigitte Hampel, Harveen Dhillon, Jeffrey Marc Zigman, et al.

► **To cite this version:**

Tim Klöckener, Simon Hess, Bengt F. Belgardt, Lars Paeger, Linda A. Verhagen, et al.. High-fat Feeding Promotes Obesity via Insulin Receptor/PI3k-Dependent Inhibition of SF-1 VMH Neurons. Nature Neuroscience, 2011, 10.1038/nn.2847 . hal-00648047

HAL Id: hal-00648047

<https://hal.science/hal-00648047>

Submitted on 5 Dec 2011

HAL is a multi-disciplinary open access archive for the deposit and dissemination of scientific research documents, whether they are published or not. The documents may come from teaching and research institutions in France or abroad, or from public or private research centers.

L'archive ouverte pluridisciplinaire **HAL**, est destinée au dépôt et à la diffusion de documents scientifiques de niveau recherche, publiés ou non, émanant des établissements d'enseignement et de recherche français ou étrangers, des laboratoires publics ou privés.

High-fat Feeding Promotes Obesity via Insulin Receptor/PI3k-Dependent Inhibition of SF-1 VMH Neurons

Tim Klöckener^{1,2,3}, Simon Hess^{2,4}, Bengt F. Belgardt^{1,2,3}, Lars Paeger^{2,4}, Linda A. W. Verhagen^{1,2,3}, Andreas Husch^{2,4}, Jong-Woo Sohn⁵, Brigitte Hampel^{1,2,3}, Harveen Dhillon⁶, Jeffrey M. Zigman⁵, Bradford B. Lowell⁶, Kevin W. Williams⁵, Joel K. Elmquist⁵, Tamas L. Horvath⁷, Peter Kloppenburg^{2,4}, Jens C. Brüning^{1,2,3}

¹ Department of Mouse Genetics and Metabolism, Institute for Genetics University of Cologne, Center for Endocrinology, Diabetes and Preventive Medicine (CEDP), University Hospital Cologne and Center for Molecular Medicine Cologne (CMMC), Zùlpicher Str. 47a, 50674 Köln, Germany

² Cologne Excellence Cluster on Cellular Stress Responses in Aging Associated Diseases (CECAD), Zùlpicher Str. 47a, 50674 Köln, Germany

³ Max-Planck-Institute for Neurological Research, Gleueler Str. 50a, 50931 Köln, Germany

⁴ Biocenter, Institute for Zoology and Center for Molecular Medicine Cologne (CMMC), University of Cologne, Zùlpicher Str. 47b, 50674 Köln, Germany

⁵ Division of Hypothalamic Research, Department of Internal Medicine, and Department of Pharmacology, University of Texas Southwestern Medical Center, Dallas, Texas 75390, USA

⁶ Beth Israel Deaconess Medical Center, Center for Life Sciences, Boston, MA 02115

⁷ Section of Comparative Medicine, Neurobiology & Departments of Obstetrics, Gynecology and Reproductive Sciences, Yale University School of Medicine, New Haven, CT 06520, USA

Running Title: Insulin action in SF-1 neurons

Address correspondence to:

Jens C. Brüning, M.D.
Institute for Genetics
Department of Mouse Genetics and Metabolism
Zùlpicher Str. 47
50674 Köln, Germany
Phone: +49-221 470 2467
Fax: +49-221 470 5185
e-mail: jens.brueining@uni-koeln.de

Abstract

SF-1-expressing neurons of the ventromedial hypothalamus (VMH) control energy homeostasis, but the role of insulin action in these cells remains undefined. We show that insulin activates PI3-kinase (PI3k) signaling in SF-1 neurons and reduces firing frequency in these cells via activation of K_{ATP} -channels. These effects are abrogated in mice with insulin receptor (IR) deficiency restricted to SF-1 neurons (SF-1^{ΔIR}-mice). While body weight and glucose homeostasis remain unaltered in SF-1^{ΔIR}-mice under normal chow diet, they exhibit protection from diet-induced leptin resistance, weight gain, adiposity and impaired glucose tolerance. High-fat feeding activates PI3k signaling in SF-1 neurons of control mice, and this response is attenuated in the VMH of SF-1^{ΔIR}-mice. Mimicking diet-induced overactivation of PI3k signaling by disruption of the PIP₃-phosphatase PTEN leads to increased body weight and hyperphagia under normal chow diet. Collectively, our experiments reveal a critical role for HFD-induced, insulin-dependent PI3k activation in VMH neurons to control energy homeostasis.

Introduction

The ventromedial nucleus of the hypothalamus (VMH) is of central importance in control of energy homeostasis. Mice lacking the steroidogenic factor (SF)-1 suffer from a failure to appropriately develop adrenal glands and gonads, and also have an abnormally developed VMH¹⁻³. These mice, when rescued from lethality by adrenal transplantation, develop massive obesity resulting from both hyperphagia and reduced energy expenditure⁴.

Regulation of VMH neurons in control of body weight includes brain-derived neurotrophic factor (BDNF), deletion of which specifically in the VMH and the adjacent dorsomedial hypothalamus (DMH) results in obesity⁵. Moreover, leptin signaling in VMH neurons significantly contributes to energy homeostasis, as SF-1 neuron specific leptin receptor disruption causes obesity^{6, 7}. VMH activity in control of glucose and energy homeostasis in turn at least in part appears to depend on glutamate release from these cells, since disruption of the vesicular glutamate transporter from SF-1 neurons causes a modest increase in body weight, when mice are exposed to HFD as well as impaired counterregulatory responses to hypoglycaemia⁸. Thus, excitatory transmission, originating from the VMH and under tight control by peripheral signals and brain-derived neuropeptides plays a central role in glucose and energy homeostasis.

However, the physiological role of insulin action on VMH neurons has not been addressed, despite the notion that unidentified VMH neurons in mice and rats can respond to insulin⁹⁻¹¹. While insulin action in the CNS regulates peripheral glucose and fat metabolism¹²⁻¹⁴ and insulin can acutely suppress food intake and decreases fat mass both in rodents and humans¹⁵⁻¹⁷, the specific neuronal population(s) mediating the anorexigenic effect of insulin are still unknown. We have previously shown that insulin signaling regulates agouti-related protein (AgRP) neurons of the arcuate nucleus (ARC) and that this effect is necessary for insulin's ability to suppress hepatic gluconeogenesis¹⁸. Thus, to directly address the

functional role of insulin action in VMH neurons, we have generated and characterized mice with disruption of the insulin receptor specifically in SF-1-expressing cells (SF-1^{ΔIR}-mice) using Cre/loxP-mediated recombination in vivo.

Results

Insulin activates PI3k in VMH neurons cell-autonomously

Since we and others have previously demonstrated that insulin-evoked PI3k signaling controls numerous critical functions in diverse neuronal populations^{10, 18-22}, we addressed whether insulin also activates this signaling pathway in SF-1-positive VMH neurons. To genetically mark SF-1-positive cells, we employed two different reporter mouse strains, which either express β -galactosidase (LacZ) or enhanced green fluorescent protein (GFP) after Cre-mediated recombination (**Fig. 1a**)^{19, 23}. We performed double immunohistochemical analysis for immunoreactive phosphatidylinositol_{3,4,5}-trisphosphate (PIP₃) and for β -galactosidase in VMH SF-1 neurons of SF-1^{LacZ}-mice, which had been fasted and either saline injected or stimulated with insulin for 10 or 20 min. This analysis revealed that insulin profoundly activates PIP₃-formation in SF-1-positive VMH neurons of control mice (**Fig. 1b, c**). Interestingly, approximately 40% of VMH SF-1 neurons exhibited strong PIP₃-immunoreactivity 20 minutes after insulin-stimulation (**Fig. 1c**). However, insulin-responsive SF-1 neurons were not uniformly distributed throughout the VMH, but clustered on both sides close to the ventricle and adjacent to the ARC, with fewer neurons showing high PIP₃ staining distal of the ventricle (data not shown). These results indicate that distinct subpopulation(s) of SF-1 neurons are insulin sensitive in control mice.

To investigate the role of insulin action in these neurons in control of energy and glucose homeostasis, we generated mice with inactivation of the insulin receptor specifically in SF-1-positive VMH cells (SF-1 ^{Δ IR}-mice). In contrast to control mice, insulin stimulation of SF-1^{LacZ: Δ IR}-mice could not increase PIP₃ levels compared to saline injection, indicating efficient deletion of IR in SF-1-neurons of SF-1 ^{Δ IR}-mice (**Fig. 1b, d**). SF-1 VMH-restricted IR deficiency was further substantiated by performing in situ hybridizations for IR-mRNA expression in the hypothalamus of control and SF-1 ^{Δ IR}-mice. While overall VMH IR-mRNA expression was reduced by 50% in the VMH of SF-1 ^{Δ IR}-mice compared to control mice (Fig.

1e), IR-mRNA expression in the neighboring DMH did not exhibit significant differences between both genotypes (data not shown). Performing double β -galactosidase immunohistochemistry and IR in situ hybridization in SF-1^{LacZ}-mice and SF-1^{LacZ:ΔIR}-mice, revealed that IR-mRNA expression was selectively reduced in β -galactosidase-positive SF-1 neurons of SF-1^{LacZ:ΔIR}-mice (**Fig. 1e**).

As insulin signaling and particularly insulin-evoked PI3k activity controls cellular growth, differentiation and survival, we assessed the numbers of β -galactosidase expressing SF-1-positive, VMH neurons using LacZ reporter mice. Lack of IR-signaling does not affect differentiation and survival of SF-1-positive VMH neurons (**Supplementary Fig. 1**).

Besides the VMH only in DNA extracts from pituitary, testis and spleen deletion of the IR-allele was detectable (data not shown), while immunoblot analyses showed unchanged IR expression in other peripheral tissues of IR^{ΔSF-1}-mice, consistent with the previously described expression pattern of SF-1 (**Fig. 1f**). Moreover, the reproductive performance of control and SF-1^{ΔIR} -mice as assessed by pregnancy interval and mating success was comparable to control mice (**Supplementary Fig. 2a, b**). Moreover, pituitary mRNA-expression of *Follicle Stimulating Hormone (FSH)*, *Luteinizing Hormone (LH)*, *Thyroid Stimulating Hormone (TSH)* and *Growth Hormone (GH)* remained unchanged SF-1^{ΔIR}-mice compared to controls (**Supplementary Fig. 2c**), also consistent with unaltered circulating concentrations of thyroid hormone in these mice (**Supplementary Fig. 2d**). Thus, IR-deficiency in SF-1-positive cells appears not to affect reproductive function in these mice.

K_{ATP} channel-dependent silencing of SF-1 neurons by insulin

Using SF-1^{GFP}-mice, we studied the effect of insulin stimulation on electrophysiological properties of SF-1 neurons in the VMH. To determine the insulin responsiveness of SF-1 neurons (SF-1^{GFP} neurons) and SF-1 neurons, which lacked the insulin receptor (SF-1^{GFP:ΔIR} neurons), we performed perforated patch clamp recordings to ensure the

integrity of intracellular components (**Fig. 2a**). The basic biophysical properties such as whole-cell capacitance, membrane potential, firing rate and input resistance were not significantly different between SF-1 neurons of both genotypes (**Table 1**). Insulin inhibited 43% (6 of 14) of the SF-1^{GFP} neurons (**Fig. 2a, c**), when recordings were performed in the mediobasal VMH, where most of the insulin-stimulated PIP₃-formation was detectable. In the subset of insulin-responsive neurons the membrane potential significantly hyperpolarized from -48.2 ± 0.7 mV to -54.1 ± 1.7 mV ($n = 6$; $p < 0.05$; **Fig. 2a, d**) and the firing rate was significantly reduced from 2.2 ± 0.5 Hz to 0.7 ± 0.5 Hz ($n = 5$; $p < 0.05$; **Fig. 2a, d**). Co-application of tolbutamide, a specific K_{ATP} channel antagonist, along with insulin resulted in the recovery of membrane potential and firing rate to control values (**Fig. 2a, d**). In contrast, none of the SF-1^{GFP:ΔIR} neurons were inhibited by insulin (0 of 12; **Fig. 2b, c, e**). Note that insulin induced excitation in one of the SF-1^{GFP} neurons and two of the SF-1^{GFP:ΔIR} neurons. Taken together, our results indicate that insulin modulates the biophysical properties in a subset of SF-1 VMH neurons in a similar manner as in POMC neurons of the arcuate nucleus of the hypothalamus (ARC)^{19,21}.

To begin to address whether potentially leptin-regulated SF-1 VMH neurons and insulin-regulated SF-1 VMH neurons might segregate into distinct populations, we performed electrophysiological recordings from identified SF-1 VMH neurons with individual or sequential application of leptin and insulin (**Supplementary tables 1–3**). This analysis revealed that SF-1 VMH neurons, which depolarized following leptin stimulation, did not decrease firing frequency upon subsequent insulin stimulation and that 3/21 neurons, which did not respond to leptin hyperpolarized upon subsequent insulin stimulation (**Supplementary Table 2**). Moreover, 1/16 neurons which failed to respond to insulin depolarized upon subsequent leptin treatment and 5/16 neurons which failed to respond to insulin hyperpolarized upon subsequent leptin application (**Supplementary table 3**).

Collectively, these experiments provide evidence that leptin and insulin responses of SF-1 VMH neurons likely segregate.

Attenuated obesity in SF-1^{ΔIR}-mice upon high-fat feeding

We investigated the effect of IR deficiency in SF-1 VMH neurons on energy homeostasis. Under normal chow-diet conditions, there was no difference in body weight, circulating plasma leptin concentrations, body fat content or epigonadal fat pad mass (**Fig. 3a–d**) between control and SF-1^{ΔIR}-mice, indicating that deletion of IR in SF-1 VMH neurons has no effect on energy homeostasis under normal chow diet conditions.

To address, whether insulin action in SF-1 VMH neurons affects energy and/or glucose homeostasis under conditions of diet-induced obesity, we analyzed control and SF-1^{ΔIR}-mice, which were exposed to high-fat diet (HFD) after weaning. This analysis revealed, that high-fat feeding clearly increased body weight, circulating plasma leptin concentrations, body fat content as well as epigonadal fat pad mass in control mice (**Fig. 3a–d**). In contrast, SF-1^{ΔIR}-mice exhibited a remarkable protection from HFD-induced weight gain (**Fig. 3a**). Interestingly, decreased HFD-induced body weight gain in SF-1^{ΔIR}-mice resulted from reduced adiposity as also serum leptin concentrations both at week 8 and at week 20 of age, body fat content as measured by nuclear magnetic resonance imaging and epigonadal fat pad mass were significantly decreased in SF-1^{ΔIR}-mice compared to controls (**Fig. 3b–d**). Consistent with reduced adiposity in these animals, adipocyte size was significantly reduced in SF-1^{ΔIR}- compared to control mice after exposure to HFD (**Fig. 3e, f**).

Improved leptin sensitivity in SF-1^{ΔIR}-mice upon high-fat feeding

As alterations in energy homeostasis can be caused by either altered energy intake, energy expenditure or a combination of both, we aimed to determine how ablation of IR-mediated signaling in the VMH attenuates high-fat diet induced weight gain and obesity. To

this end, we determined food intake as well as O₂ consumption and CO₂ production via indirect calorimetry in 6- to 7-week-old and 12- to 13-week-old control and SF-1^{ΔIR}-mice exposed to HFD. This analysis revealed, that food intake of young SF-1^{ΔIR}-mice prior to the onset of alterations in body weight was not different from control mice (**Fig. 4a**), whereas older SF-1^{ΔIR}-mice exhibited a significant reduction of absolute caloric intake compared to controls (**Fig. 4b**). However, this difference was not obvious, when caloric intake was normalized for altered body weight (**Supplementary Fig. 3**). On the other hand, O₂ consumption (**Fig. 4c, d**), CO₂ production (data not shown) and locomotor activity (data not shown) did not differ between young or older SF-1^{ΔIR} and control mice, when exposed to high-fat diet. Similarly, the respiratory exchange rate (RER) remained unchanged in SF-1^{ΔIR}-mice (data not shown).

To directly address, whether IR deletion from SF1 VMH neurons alters leptin sensitivity, we assessed the efficiency of intracerebroventricularly (i.c.v.) administered leptin to inhibit food intake in control and SF-1^{ΔIR}-mice exposed to HFD. Importantly, these studies were performed in 8-week-old animals prior to the onset of potentially confounding alterations in fat and body mass (data not shown). This analysis revealed a significant increase in leptin sensitivity in SF-1^{ΔIR}-mice compared to controls (**Fig. 4e**).

Improved glucose metabolism in SF-1^{ΔIR}-mice upon high-fat feeding

Since we and others have previously demonstrated that insulin action in the CNS regulates peripheral glucose metabolism^{14, 18, 24, 25} and that diet-induced attenuation of insulin action in the CNS contributes to the development of impaired glucose metabolism^{26, 27}, we investigated the role of insulin action in SF-1 VMH neurons in control of peripheral glucose metabolism. Analysis of blood glucose concentrations, plasma insulin concentrations, insulin and glucose tolerance tests revealed no major alterations of glucose metabolism in the absence of insulin signaling in the VMH under normal chow diet conditions (**Supplementary Fig. 4a–**

d). Although upon high-fat diet exposure blood glucose levels did not differ (**Fig. 5a**), SF-1^{ΔIR}-mice exhibited significantly reduced plasma insulin concentrations compared to control mice (**Fig. 5b**). Moreover, SF-1^{ΔIR}-mice fed a high-fat diet exhibited significantly improved insulin and glucose tolerance as compared to control mice exposed to HFD (**Fig. 5c, d**). Collectively, these data indicate that insulin signaling in SF-1 VMH neurons does not directly regulate peripheral glucose metabolism, but that protection from diet-induced obesity in SF-1^{ΔIR}-mice leads to slightly improved glucose metabolism in these mice upon high-fat feeding.

Increased PIP₃ formation in the VMH promotes weight gain

Since abrogation of IR signaling in SF-1 VMH neurons reduces obesity development, we asked whether insulin-dependent signaling might be overactivated in the VMH under conditions of obesity. To this end, we analyzed activation of PI3k signaling in the VMH in control mice under conditions of high-fat feeding. Strikingly, control mice exposed to high-fat diet exhibited a clear increase in immunoreactive PIP₃ even after an overnight fast compared to lean mice (**Fig. 6a, Fig. 1c**). While in lean mice, only 10% of SF-1 neurons exhibited high PIP₃ immunoreactivity (**Fig. 1c**), this proportion was increased to 40% in control mice exposed to high-fat diet (**Fig. 6a**). This increase in SF-1 cells exhibiting massive PIP₃ accumulation was significantly attenuated in SF-1^{ΔIR}-mice (**Fig. 6a**). On the other hand, the percentage of SF-1 VMH neurons exhibiting moderate PIP₃ immunoreactivity was increased in HFD-exposed SF-1^{ΔIR}-mice compared to controls (**Fig. 6a**), indicating some residual diet-induced activation of PI3k signaling in SF-1 VMH neurons, even in the absence of IR signaling. These experiments clearly indicate that high-fat diet feeding massively increases PI3k activity in SF-1 VMH neurons and that this activation to significant proportion depends on IR signaling in these neurons.

To further functionally address the importance of diet-induced, insulin-dependent overactivation of PI3k signaling in the VMH, we aimed to mimic this effect through genetic

PI3k overactivation *in vivo*. The Phosphatase and Tensin Homolog (PTEN) negatively regulates PI3k signaling by dephosphorylating PIP₃ to PIP₂, thus, deletion of PTEN leads to accumulation of PIP₃ and subsequent hyperactivation of the PI3k pathway^{19,28}. Therefore, we crossed mice carrying a loxP-flanked PTEN allele with SF-1 Cre mice and further intercrossing of the offspring resulted in the generation of VMH-specific PTEN knockout mice, i.e. SF-1^{ΔPTEN}-mice and the respective controls. Compared to control mice, deletion of PTEN increased the number of SF-1 neurons with moderate to high levels of PIP₃ when the mice were fed normal chow (**Fig. 6b**). Thus, SF-1 VMH neuron-restricted PTEN deletion mimics diet-induced overactivation of PI3k signaling in these neurons.

Next we aimed to assess the consequence of increased PIP₃ formation in SF-1 neurons on body weight and caloric intake. This analysis revealed a significant increase of body weight and food intake in SF-1^{ΔPTEN}-mice compared to control mice exposed to normal chow diet (**Fig. 6c, d**). However, when exposed to HFD, these animals developed the same degree of obesity as obese control mice exposed to HFD (**Fig. 6c**). These experiments indicate that PI3k overactivation in SF-1 neurons contributes to the weight gain and hyperphagia associated with high-fat feeding.

To directly address the contribution of impaired PI3k activation in SF-1 neurons of SF-1^{ΔIR}-mice to the protection of these mice from the development of diet induced obesity, we generated mice lacking both IR and PTEN in SF-1 neurons, i.e. SF-1^{ΔIR:ΔPTEN}-mice. Comparing body weight (**Fig. 6c**), epigonadal fat mass (**Fig. 6e**), body fat content (**Fig. 6f**) and adipocyte size (**Fig. 6g**) in control and SF-1^{ΔIR:ΔPTEN}-mice exposed to high-fat diet revealed that protection from diet-induced weight gain and obesity in SF-1^{ΔIR}-mice can be abrogated by simultaneous deletion of PTEN in these neurons. Collectively, these experiments indicate, that insulin-stimulated overactivation of PI3k signaling in SF-1 VMH neurons plays an important role in the development of high-fat diet-induced obesity.

Increased activity of POMC neurons in SF-1^{ΔIR}-mice

To further investigate the molecular basis of altered body weight regulation in SF-1^{ΔIR}-mice, we analyzed the expression of hypothalamic neuropeptides critically involved in control of energy homeostasis²⁹⁻³⁴. However, neither expression of ARC-derived neuropeptides in the melanocortin pathway (*POMC*, *AgRP*) nor that of *cocaine and amphetamine regulated transcript* (*CART*) or *neuropeptide Y* (*NPY*) exhibited altered expression dependent on IR expression in SF-1 VMH neurons (**Fig. 7a**). Moreover, expression of *SF-1* and *BDNF* remained unchanged (**Fig. 7b**). Thus, changes in expression of the investigated gene products do not explain the metabolic phenotype observed in mice lacking IR in SF-1 neurons.

Since VMH neurons located in the mediobasal VMH have been described to provide glutamatergic innervation of anorexigenic POMC neurons in the ARC³⁵, we investigated whether altering insulin action in SF-1 VMH neurons may affect electrical activity of POMC neurons upon high-fat feeding. To this end we performed electrophysiological recording from genetically marked, GFP-expressing POMC neurons⁴¹ in control (POMC^{GFP}) and SF-1^{ΔIR}-mice (POMC^{GFP}; SF-1^{ΔIR}) after exposure to HFD, which revealed that exposure to HFD impaired neuronal activity of POMC neurons. In HFD control mice mean firing frequency of POMC neurons was 1 Hz and more than half of the neurons did not exhibit spontaneous action potentials (**Fig. 7c, d, e**). In contrast, mean firing frequency of POMC neurons of SF-1^{ΔIR}-mice was increased to 2.7 Hz, and the proportion of silent POMC-neurons was reduced to 25%, despite exposure to HFD. Taken together, these experiments indicate, that abrogation of IR signaling from SF-1 VMH neurons increases activity of anorexigenic POMC neurons under HFD.

Discussion

Numerous studies over the last decades have established the VMH as an important satiety “center”^{6, 36, 37}. The signals controlling VMH neuron activity are increasingly well defined, partly through the use of novel techniques including those of targeted transgenesis and cell-type specific knockout mice^{1, 4, 6, 8}. Thus, abrogation of leptin signaling in SF-1-positive VMH neurons causes obesity and VMH-restricted alterations of BDNF affect energy homeostasis, supporting the notion that activation of glutamatergic SF-1 VMH neurons is critical for the suppression of feeding^{5-7, 37}. Finally, insulin and also nutrients such as glucose have been previously demonstrated to control VMH neuronal activity, however, the physiological importance of this regulation remained unclear as of now. The present study establishes that deletion of the insulin receptor gene and subsequent inactivation of insulin-stimulated signaling provides partial protection from high-fat diet-induced hyperphagia, weight gain and obesity.

From a mechanistic point of view, our study identifies insulin as a crucial regulator of neuronal excitability, via PI3k-dependent activation of K_{ATP} channels, as insulin’s ability to inhibit firing of SF-1-positive VMH neurons is abrogated by tolbutamide. The majority of insulin-responsive neurons are clustered in an area in the mediobasal VMH. Interestingly, the same area provides glutamatergic innervations to anorexigenic POMC neurons in the ARC as revealed by photoactivated, glutamate-uncaging mapping³⁵. Thus, we propose, that overactivated insulin signaling in the VMH as present under high-fat diet conditions inhibits glutamatergic projections to POMC neurons. This notion is consistent with the observed increase of POMC cell firing in SF-1^{ΔIR}-mice, when the mice are exposed to HFD.

Interestingly, under normal chow diet, insulin-dependent silencing of these cells appears not to occur because SF-1^{ΔIR}-mice are phenotypically indistinguishable from controls under these conditions. Only when insulin levels rise, as upon high-fat feeding, insulin action

appears to reach a threshold for profound PI3k activation, subsequent K_{ATP} channel activation and ultimately neuronal silencing. This notion is directly supported by two findings of the present study. First, high-fat feeding results in increased PIP_3 formation, and second this increase can be significantly attenuated by abrogation of IR signaling in VMH neurons. These experiments reveal that there appears to exist a relatively high threshold for PI3k-dependent K_{ATP} channel activation. This is consistent with our previous findings in POMC neurons where profound PI3k activation - either following insulin stimulation or via genetic ablation of the PIP_3 phosphatase PTEN - activate K_{ATP} channels to cause neuronal silencing. On the other hand, leptin stimulates PI3k signaling to much lesser extent and thus fails to activate K_{ATP} channels but rather promotes POMC cell firing via activation of unspecific cation channels^{19, 38, 39}. The differential threshold for insulin's and leptin's ability to activate apparently also holds true for VMH neurons, as insulin silences these cells, while leptin promotes firing in the majority of SF-1 VMH neurons⁶; it has also been demonstrated that PI3k signaling in SF-1 cells is critical for leptin's ability to increase firing⁴⁰.

Another important finding of the present study is that while high-fat feeding has been demonstrated to cause insulin resistance in the arcuate nucleus of the hypothalamus⁴¹, increased insulin action in the VMH upon high-fat feeding indicates that regional differences appear within the hypothalamus ranging from resistance to enhanced basal signaling under conditions of diet-induced obesity. This novel finding of differentially regulated insulin sensitivity within the hypothalamus may stem from differences in insulin accessibility of the neurons in these different locations. While the blood brain barrier in the ARC is highly permeable⁴², POMC and AgRP neurons may sense elevated circulating insulin concentrations, which lead to signal desensitization. Indeed, it could be demonstrated in cultured POMC neurons, that chronic insulin stimulation results in signal attenuation via activation of proteasome-mediated IRS degradation^{42, 43}. On the other hand, VMH neurons

may be exposed to elevated, but relatively lower insulin concentrations than ARC neurons leading to increased tonic insulin signaling. Alternatively, we and others have recently demonstrated that fatty acids can cause leptin and insulin resistance in ARC neurons via TLR-dependent activation of inflammatory signaling²⁶. Differential accessibility of VMH neurons to circulating fatty acids may prevent that insulin resistance in response to high-fat feeding occurs in this anatomical localization. Whatever the molecular basis for this phenomenon is, our experiments reveal an intriguing concept, that differential, nucleus-specific dysregulation of insulin action upon high-fat feeding, i.e. insulin resistance in POMC neurons and overactivation of insulin action in the VMH can cooperate to cause obesity.

Insulin stimulation enhances production of PIP₃, which will subsequently bind to and open K_{ATP} channels, resulting in neuronal silencing. However, in POMC neurons leptin- and insulin-stimulated PI3k activation is also required for POMC transcription and neuropeptide synthesis in a FOXO1-dependent manner^{19, 21, 44}. In contrast to this, mice lacking the principle PIP₃-activated downstream kinase, PDK1, in SF-1 cells, were neither protected nor more sensitive to diet-induced obesity and hyperglycemia (BFB and JCB, unpublished observations), indicating that in SF-1 neurons insulin primarily regulates neuronal activity and thus neurotransmitter/neuropeptide release from these cells.

Taken together, using multiple complementary mouse models, we demonstrate that high-fat feeding-induced hyperinsulinemia leads to cell autonomous hyperpolarization of SF-1 neurons, leading to functional changes in the synaptic input onto POMC neurons, causing obesity and glucose intolerance.

Methods

Animal care

Care of all animals was within institutional animal care committee guidelines. All animal procedures were conducted in compliance with protocols and approved by local government authorities (Bezirksregierung Köln, Cologne, Germany). Mouse husbandry, genotyping and diet followed previously described methods¹⁸. All alleles had been backcrossed for at least 4 generations onto a C57BL/6 background. Cre-negative littermates were used as controls at all times except for reporter mouse studies. The genetic background was unchanged throughout all experiments.

Food intake

Daily food intake was calculated as the average intake of normal chow or high-fat diet during two weeks. Mice were acclimated to the food intake settings for at least five days.

Gene expression analysis

RNA extraction and gene expression was analyzed using quantitative RT-PCR as previously described²⁷. Probes for target genes were from TaqMan Assay-on-Demand kits (Applied Biosystems). Samples were adjusted for total RNA content by transferrin receptor or beta-glucuronidase.

Analytical procedures

Blood glucose values were determined from whole venous blood using an automatic glucose monitor (GlucoMen; A. Menarini Diagnostics). Serum insulin and leptin levels were measured by ELISA using mouse standards according to the manufacturer's guidelines

(Mouse Leptin ELISA, 90030, Crystal Chem., Downers Grove, IL, USA; Rat Insulin ELISA, INSKR020, Crystal Chem., Downers Grove, IL, USA).

Glucose and insulin tolerance tests

Glucose and insulin tolerance tests were performed as described previously¹³.

Indirect calorimetry

Oxygen consumption, CO₂ production and locomotor activity was measured over a period of 3 days as described previously²⁶.

Leptin sensitivity

Icv cannulas were implanted as previously described⁴⁵, except that the lateral ventricle was targeted using coordinates located using a Brain Atlas (coordinates were bregma 1.0 mm lateral, 0.2 mm caudal, and 2.0 mm ventral). After recovery and an overnight fast, mice were injected with 2 μ L artificial cerebrospinal fluid (ACSF). Food intake was measured 4 and 8 hours later. After a 7-day break, 5 μ g/2ml mouse leptin (NHPP) was injected and food intake was measured 4 and 8 hours later. Based on the notion that SF-1 ^{Δ IR}-mice are protected from HFD-induced obesity, data were analyzed by unpaired, one-tailed Student's *t*-test.

Western blotting

Indicated tissues were dissected and homogenized in homogenization buffer with a polytron homogenizer (IKA Werke), and Western blot analyses were performed by standard methods with antibodies raised against IR- β (sc-711, Santa Cruz) as previously described³³.

Immunohistochemistry

SF-1 Cre^{+/-} mice were mated with RosaArte1 mice¹⁹ or Z/EG mice to generate SF-1^{LacZ} and SF-1^{GFP} mice which served as controls for the immunohistochemistry and electrophysiology studies, respectively. SF-1^{ΔIR}-mice were mated with RosaArte1 mice¹⁹ or Z/EG mice to generate SF-1^{LacZ:ΔIR} and SF-1^{GFP:ΔIR} mice which lack the insulin receptor in SF-1-expressing cells but express lacZ or GFP in these cells, respectively. For GFP stainings, mice were perfused with saline solution followed by 4% paraformaldehyde (PFA) in 0.1 M phosphate-buffered saline (PBS; pH 7.4). Hypothalami were dissected, postfixed in 4% PFA at 4°C, transferred to 20% sucrose for 6 hours, and frozen in tissue freezing medium. Then, 25 μm thick free-floating coronal sections were cut through the ARC using a freezing microtome (Leica, Germany). The sections were collected in PBS/azide (pH 7.4) and washed extensively to remove cryoprotectant. The sections were stained as previously described, using rabbit anti-GFP antibody at a 1:10000 dilution (A6455 from Invitrogen/Molecular Probes, Karlsruhe, Germany)⁴⁶.

For PIP₃/lacZ double stainings, SF-1^{LacZ} control and SF-1^{LacZ:ΔIR} reporter mice were perfused transcardially with physiologic saline solution, frozen in tissue freezing medium (Jung, Leica Instruments, Germany), and sectioned on a cryostat. Stainings were performed and analyzed as previously described^{19,21}.

Combined in situ hybridisation and immunohistochemistry

For *in situ* hybridisation combined with immunohistochemistry, series of 8 μm coronal sections of freshly frozen brains were sliced using a cryostat, thaw-mounted onto RNase free slides and stored at -80°C until processing. Locked Nucleic Acid (LNATM) RNA probe detecting exon 4 of the IR gene labelled at the 5' and 3' end with digoxigenin (DIG) was supplied by Exiqon Inc. For *in situ* hybridisation, brain sections containing the VMH were proper fixed onto slides in 4% ice-cold paraformaldehyde (w/v in PBS). Acetylation (5 μl/ml

acetic anhydride in 0.1M triethanoleamine) reduced unspecific background signals. In an initial step (prehybridisation), the slides were immersed in hybridisation buffer (50% deionised formamide; 1× Denhardt’s solution; 500 µg/ml salmon sperm DNA; 500 µg/ml t-RNA) for 2.5 h at 48 °C to block unspecific binding. Hybridisation was performed for at least 6 h at 48 °C in hybridisation buffer containing 10% dextran sulphate. Subsequently, washes with increased stringency were performed. To further remove unbound LNA™ probe, the brain slices were subjected to RNase A (0.5 µl/ml) digestion. In addition to block unspecific staining, slices were treated with 3% H₂O₂ in TBS and Tyramide Blocking solution, subsequently. Specifically bound probe was detected using a digoxigenin-antibody coupled to peroxidase with Cyanine 3 Fluorophore Tyramide. Following *in situ* hybridisation, immunohistochemistry for detection of LacZ positive neurons was performed as described before ²¹. Finally, slides were covered up with DAPI Vector Mounting Shield to visualize neurons. Pictures were taken using the Zeiss Meta Confocal microscope.

Quantification of the insulin receptor signal was performed with ImageJ (NIH) by converting the Cyanine 3 Fluorophore Tyramide signal into grey scale and measuring mean grey values of the VMH in SF-1^{LacZ} and SF-1^{LacZ:ΔIR} mice, using the LacZ signal as marker for the VMH. During these measurements the area was kept constant by using the *specify ROI* plugin.

Electrophysiology

Insulin response experiments were performed on brain slices from 21- to 28-day old female and male SF-1^{GFP} and SF-1^{GFP:ΔIR} mice that expressed green fluorescent protein (eGFP) selectively in SF-1 neurons. Basic firing frequency measurements of POMC neurons were performed in 15- to 20-week-old transgenic mice, expressing the green fluorescent protein under control of the POMC promotor, either in control (IR^{fl/fl}) background

(POMC^{GFP}) or in mice lacking the insulin receptor in SF-1 expressing cells (POMC^{GFP};SF-1^{ΔIR}) upon HFD exposure. The animals were anesthetized with halothane (B4388; Sigma-Aldrich, Taufkirchen, Germany) and decapitated. Coronal slices (250 – 300 μm) containing the ventromedial hypothalamus (VMH) and the arcuate nucleus (ARC) were cut with a vibration microtome (HM-650 V; Thermo Scientific, Walldorf, Germany) under cold (4°C), carbogenated (95% O₂ and 5% CO₂), glycerol-based modified artificial cerebrospinal fluid GaCSF; ⁴⁷. GaCSF contained (in mM): 250 glycerol, 2.5 KCl, 2 MgCl₂, 2 CaCl₂, 1.2 NaH₂PO₄, 10 HEPES, 21 NaHCO₃, 5 glucose adjusted to pH 7.2 with NaOH.

If not mentioned otherwise, during the recordings the slices were continuously superfused with carbogenated aCSF at a flow rate of ~2 ml·min⁻¹. aCSF contained (in mM): 125 NaCl, 2.5 KCl, 2 MgCl₂, 2 CaCl₂, 1.2 NaH₂PO₄, 21 NaHCO₃, 10 HEPES, and 5 glucose adjusted to pH 7.2 with NaOH. Patch-clamp recordings were performed at room temperature with an EPC10 patch-clamp amplifier (HEKA, Lambrecht, Germany). Data were sampled at intervals of 100 μs (10 kHz) and low-pass filtered at 2 kHz with a four-pole Bessel filter. Whole-cell capacitance was determined by using the capacitance compensation (C-slow) of the EPC10. Cell input resistances (R_M) were calculated from voltage responses to hyperpolarizing current pulses. The calculated liquid junction potential (14.6 mV) between intracellular and extracellular solution was not compensated.

Current clamp recordings in the perforated patch configuration were performed using protocols modified from Horn and Marty ⁴⁸ and Akaike and Harata ⁴⁹. The recordings were performed with ATP and GTP free pipette solution containing (in mM): 128 K-gluconate, 10 KCl, 10 HEPES, 0.1 EGTA, 2 MgCl₂ and adjusted to pH 7.3 with KOH. The patch pipette was tip filled with internal solution and back filled with amphotericin B- (~200 μg·ml⁻¹; A4888; Sigma) or nystatin-containing (~200 μg·ml⁻¹; N6261; Sigma) internal solution to achieve perforated patch recordings. Nystatin was dissolved in methanol (final concentration:

2%) according to the instructions of Akaike et al.⁴⁹ and amphotericin B was dissolved in dimethyl sulfoxide (final concentration: 0.4 – 0.5%; D8418, Sigma; DMSO). Either substance was added to the modified pipette solution shortly before use. The DMSO and methanol concentrations had no obvious effect on the investigated neurons. During the perforation process access resistance (R_a) was constantly monitored and experiments were started after R_a had reached steady state (~15 – 20 min) and the action potential amplitude was stable. To check the integrity of the perforated patch, we monitored R_a and GFP fluorescence of the neurons. For each recording, the firing rate (or baseline membrane potential) averaged from 30 s intervals were taken as single data points. 10 data points were taken to calculate the mean with standard deviation (SD) before and during insulin application.

Drugs were bath-applied at a flow rate of ~2 ml·min⁻¹. Insulin (200 nM; I9278; Sigma) was added to the normal aCSF shortly before the experiments. The K_{ATP} channel blocker tolbutamide (200 μM; T0891, Sigma) was dissolved in DMSO and added to the normal aCSF with a final DMSO concentration of 0.25%. The DMSO concentration had no obvious effect on the investigated neurons.

Data analysis was performed with Igor Pro 6 (Wavemetrics, Lake Oswego, OR, USA) and Graphpad Prism (version 5.0b; Graphpad Software Inc., La Jolla, CA, USA). Data are given as mean ± standard error. We found that the basic firing properties of SF-1 neurons and their insulin responsiveness were not homogenous. Therefore, we used the “3 times standard deviation” criterion and a neuron was considered insulin-responsive if the change in membrane potential induced by insulin was 3 times larger than the standard deviation, see^{6, 50}. To determine differences in means between treatments, one-way ANOVA was performed; *post hoc* pairwise comparisons were performed using *t*-tests with the Newman-Keuls method for *p* value adjustment. For analysis of firing properties of POMC neurons in HFD-fed

control and SF-1^{ΔIR} mice, based on the observed protection from HFD-induced obesity in the latter mice and the predicted improvement of anorexigenic neuronal activity, an unpaired one-tailed Student's *t*-test was performed. POMC neurons with a firing frequency of <0.5Hz were classified as silent. A significance level of 0.05 was accepted for all tests.

Acknowledgments

We thank G. Schmall and T. Rayle for excellent secretarial assistance and S. Irlenbusch, and H. Wratil for outstanding technical assistance. We thank the Ed Parlow (NHPP) for providing recombinant murine leptin and Malcolm Low for providing POMC^{GFP}-mice. This work was supported by grants from the DFG (KL 762/2-2 to P.K.), ZMMK, under FP7- HEALTH-2009- 241592 (European Union) EurOCHIP, and under FP7-KBBE-2010-4 – 266408 (European Union) Full4Health and through the “Kompetenznetz Adipositas (Competence Network for Adipositas)” funded by the Federal Ministry of Education and Research (FKZ 01GI0845) to J.C.B., and the DFG (Br. 1492/7-1) to J.C.B. This work was supported by National Institute of Health Grants R01DK53301 and RL1DK081185, (to J.K.E.), and K01DK087780 (to K.W.W.). This work was also supported by PL1 DK081182 and UL1RR024923 as well as K08 DK068069-01A2 (to J.M.Z.).

Author Contribution

T.K., S.H., B.F.B., L.P., L.A.W.V., A.H., J.W.S., B.H., T.L.H. performed experiments, analyzed data and contributed to writing the paper. H.D., J.M.Z., B.B.L., K.W.W., J.K.E. provided unique reagents and transgenic mice for this study. P.K. analyzed data and contributed to writing the paper. T.K., J.C.B. conceptualized the study and wrote the manuscript. All authors read and agreed on the final version of the manuscript.

References

1. Ikeda, Y., Luo, X., Abbud, R., Nilson, J.H. & Parker, K.L. The nuclear receptor steroidogenic factor 1 is essential for the formation of the ventromedial hypothalamic nucleus. *Mol Endocrinol* **9**, 478-486 (1995).
2. Sadovsky, Y., *et al.* Mice deficient in the orphan receptor steroidogenic factor 1 lack adrenal glands and gonads but express P450 side-chain-cleavage enzyme in the placenta and have normal embryonic serum levels of corticosteroids. *Proceedings of the National Academy of Sciences of the United States of America* **92**, 10939-10943 (1995).
3. Shinoda, K., *et al.* Developmental defects of the ventromedial hypothalamic nucleus and pituitary gonadotroph in the Ftz-F1 disrupted mice. *Dev Dyn* **204**, 22-29 (1995).
4. Majdic, G., *et al.* Knockout mice lacking steroidogenic factor 1 are a novel genetic model of hypothalamic obesity. *Endocrinology* **143**, 607-614 (2002).
5. Unger, T.J., Calderon, G.A., Bradley, L.C., Sena-Esteves, M. & Rios, M. Selective deletion of Bdnf in the ventromedial and dorsomedial hypothalamus of adult mice results in hyperphagic behavior and obesity. *J Neurosci* **27**, 14265-14274 (2007).
6. Dhillon, H., *et al.* Leptin directly activates SF1 neurons in the VMH, and this action by leptin is required for normal body-weight homeostasis. *Neuron* **49**, 191-203 (2006).
7. Bingham, N.C., Anderson, K.K., Reuter, A.L., Stallings, N.R. & Parker, K.L. Selective loss of leptin receptors in the ventromedial hypothalamic nucleus results in increased adiposity and a metabolic syndrome. *Endocrinology* **149**, 2138-2148 (2008).
8. Tong, Q., *et al.* Synaptic glutamate release by ventromedial hypothalamic neurons is part of the neurocircuitry that prevents hypoglycemia. *Cell metabolism* **5**, 383-393 (2007).
9. Davidowa, H. & Plagemann, A. Inhibition by insulin of hypothalamic VMN neurons in rats overweight due to postnatal overfeeding. *Neuroreport* **12**, 3201-3204 (2001).
10. Spanswick, D., Smith, M.A., Mirshamsi, S., Routh, V.H. & Ashford, M.L. Insulin activates ATP-sensitive K⁺ channels in hypothalamic neurons of lean, but not obese rats. *Nature neuroscience* **3**, 757-758 (2000).
11. Cotero, V.E. & Routh, V.H. Insulin blunts the response of glucose-excited neurons in the ventrolateral-ventromedial hypothalamic nucleus to decreased glucose. *American journal of physiology* **296**, E1101-1109 (2009).
12. Gelling, R.W., *et al.* Insulin action in the brain contributes to glucose lowering during insulin treatment of diabetes. *Cell metabolism* **3**, 67-73 (2006).
13. Bruning, J.C., *et al.* Role of brain insulin receptor in control of body weight and reproduction. *Science (New York, N.Y)* **289**, 2122-2125 (2000).
14. Koch, L., *et al.* Central insulin action regulates peripheral glucose and fat metabolism in mice. *The Journal of clinical investigation* **118**, 2132-2147 (2008).
15. Niswender, K.D., *et al.* Insulin activation of phosphatidylinositol 3-kinase in the hypothalamic arcuate nucleus: a key mediator of insulin-induced anorexia. *Diabetes* **52**, 227-231 (2003).
16. Hallschmid, M., *et al.* Intranasal insulin reduces body fat in men but not in women. *Diabetes* **53**, 3024-3029 (2004).
17. Obici, S., Feng, Z., Karkanias, G., Baskin, D.G. & Rossetti, L. Decreasing hypothalamic insulin receptors causes hyperphagia and insulin resistance in rats. *Nature neuroscience* **5**, 566-572 (2002).
18. Konner, A.C., *et al.* Insulin action in AgRP-expressing neurons is required for suppression of hepatic glucose production. *Cell metabolism* **5**, 438-449 (2007).
19. Plum, L., *et al.* Enhanced PIP3 signaling in POMC neurons causes KATP channel activation and leads to diet-sensitive obesity. *J Clin Invest* **116**, 1886-1901 (2006).

20. Plum, L., *et al.* Enhanced leptin-stimulated Pi3k activation in the CNS promotes white adipose tissue transdifferentiation. *Cell metabolism* **6**, 431-445 (2007).
21. Belgardt, B.F., *et al.* PDK1 deficiency in POMC-expressing cells reveals FOXO1-dependent and -independent pathways in control of energy homeostasis and stress response. *Cell metabolism* **7**, 291-301 (2008).
22. Choudhury, A.I., *et al.* The role of insulin receptor substrate 2 in hypothalamic and beta cell function. *J Clin Invest* **115**, 940-950 (2005).
23. Novak, A., Guo, C., Yang, W., Nagy, A. & Lobe, C.G. Z/EG, a double reporter mouse line that expresses enhanced green fluorescent protein upon Cre-mediated excision. *Genesis* **28**, 147-155 (2000).
24. Obici, S., Zhang, B.B., Karkanias, G. & Rossetti, L. Hypothalamic insulin signaling is required for inhibition of glucose production. *Nat Med* **8**, 1376-1382 (2002).
25. Pocai, A., *et al.* Hypothalamic K(ATP) channels control hepatic glucose production. *Nature* **434**, 1026-1031 (2005).
26. Kleinridders, A., *et al.* MyD88 signaling in the CNS is required for development of fatty acid-induced leptin resistance and diet-induced obesity. *Cell metabolism* **10**, 249-259 (2009).
27. Belgardt, B.F., *et al.* Hypothalamic and pituitary c-Jun N-terminal kinase 1 signaling coordinately regulates glucose metabolism. *Proc Natl Acad Sci U S A* [**Epub ahead of print**] (2010).
28. Maehama, T. & Dixon, J.E. The tumor suppressor, PTEN/MMAC1, dephosphorylates the lipid second messenger, phosphatidylinositol 3,4,5-trisphosphate. *The Journal of biological chemistry* **273**, 13375-13378 (1998).
29. Fan, W., Boston, B.A., Kesterson, R.A., Hruby, V.J. & Cone, R.D. Role of melanocortinergic neurons in feeding and the agouti obesity syndrome. *Nature* **385**, 165-168 (1997).
30. Li, G., Mobbs, C.V. & Scarpace, P.J. Central pro-opiomelanocortin gene delivery results in hypophagia, reduced visceral adiposity, and improved insulin sensitivity in genetically obese Zucker rats. *Diabetes* **52**, 1951-1957 (2003).
31. Asnicar, M.A., *et al.* Absence of cocaine- and amphetamine-regulated transcript results in obesity in mice fed a high caloric diet. *Endocrinology* **142**, 4394-4400 (2001).
32. McMinn, J.E., Wilkinson, C.W., Havel, P.J., Woods, S.C. & Schwartz, M.W. Effect of intracerebroventricular alpha-MSH on food intake, adiposity, c-Fos induction, and neuropeptide expression. *Am J Physiol Regul Integr Comp Physiol* **279**, R695-703 (2000).
33. Gropp, E., *et al.* Agouti-related peptide-expressing neurons are mandatory for feeding. *Nature neuroscience* **8**, 1289-1291 (2005).
34. Clark, J.T., Sahu, A., Kalra, P.S., Balasubramaniam, A. & Kalra, S.P. Neuropeptide Y (NPY)-induced feeding behavior in female rats: comparison with human NPY ([Met17]NPY), NPY analog ([norLeu4]NPY) and peptide YY. *Regul Pept* **17**, 31-39 (1987).
35. Sternson, S.M., Shepherd, G.M. & Friedman, J.M. Topographic mapping of VMH --> arcuate nucleus microcircuits and their reorganization by fasting. *Nature neuroscience* **8**, 1356-1363 (2005).
36. Marshall, N.B. & Mayer, J. Specificity of gold thioglucose for ventromedial hypothalamic lesions and hyperphagia. *Nature* **178**, 1399-1400 (1956).
37. Xu, B., *et al.* Brain-derived neurotrophic factor regulates energy balance downstream of melanocortin-4 receptor. *Nat Neurosci* **6**, 736-742 (2003).
38. Hill, J.W., *et al.* Acute effects of leptin require PI3K signaling in hypothalamic proopiomelanocortin neurons in mice. *The Journal of clinical investigation* **118**, 1796-1805 (2008).
39. Cowley, M.A., *et al.* Leptin activates anorexigenic POMC neurons through a neural network in the arcuate nucleus. *Nature* **411**, 480-484 (2001).

40. Xu, Y., *et al.* PI3K signaling in the ventromedial hypothalamic nucleus is required for normal energy homeostasis. *Cell Metab* **12**, 88-95.
41. Schubert, M., *et al.* Role for neuronal insulin resistance in neurodegenerative diseases. *Proceedings of the National Academy of Sciences of the United States of America* **101**, 3100-3105 (2004).
42. Mullier, A., Bouret, S.G., Prevot, V. & Dehouck, B. Differential distribution of tight junction proteins suggests a role for tanycytes in blood-hypothalamus barrier regulation in the adult mouse brain. *J Comp Neurol* **518**, 943-962 (2010).
43. Mayer, C.M. & Belsham, D.D. Palmitate attenuates insulin signaling and induces endoplasmic reticulum stress and apoptosis in hypothalamic neurons: rescue of resistance and apoptosis through adenosine 5' monophosphate-activated protein kinase activation. *Endocrinology* **151**, 576-585 (2010).
44. Plum, L., *et al.* The obesity susceptibility gene *Cpe* links FoxO1 signaling in hypothalamic pro-opiomelanocortin neurons with regulation of food intake. *Nat Med* **15**, 1195-1201 (2009).
45. Brown, L.M., Clegg, D.J., Benoit, S.C. & Woods, S.C. Intraventricular insulin and leptin reduce food intake and body weight in C57BL/6J mice. *Physiol Behav* **89**, 687-691 (2006).
46. Janoschek, R., *et al.* gp130 signaling in proopiomelanocortin neurons mediates the acute anorectic response to centrally applied ciliary neurotrophic factor. *Proceedings of the National Academy of Sciences of the United States of America* **103**, 10707-10712 (2006).
47. Ye, J.H., Zhang, J., Xiao, C. & Kong, J.Q. Patch-clamp studies in the CNS illustrate a simple new method for obtaining viable neurons in rat brain slices: glycerol replacement of NaCl protects CNS neurons. *J Neurosci Methods* **158**, 251-259 (2006).
48. Horn, R. & Marty, A. Muscarinic activation of ionic currents measured by a new whole-cell recording method. *J Gen Physiol* **92**, 145-159 (1988).
49. Akaike, N. & Harata, N. Nystatin perforated patch recording and its applications to analyses of intracellular mechanisms. *Jpn J Physiol* **44**, 433-473 (1994).
50. Kloppenburg, P., Zipfel, W.R., Webb, W.W. & Harris-Warrick, R.M. Heterogeneous effects of dopamine on highly localized, voltage-induced Ca²⁺ accumulation in identified motoneurons. *J Neurophysiol* **98**, 2910-2917 (2007).

Figure Legends

Figure 1. Insulin action in VMH neurons and generation of IR^{ΔSF-1}-mice.

a) SF-1 Cre-mediated recombination was visualized by immunohistochemistry for GFP in brains of SF-1^{GFP} mice. A representative section is shown.

b) Double immunohistochemistry for lacZ and PIP₃ of ventromedial hypothalamic neurons of SF-1^{LacZ} and SF-1^{LacZ:ΔIR} reporter mice was performed in overnight-fasted animals, which were intravenously injected with either saline or insulin and sacrificed 10 or 20 min after stimulation. A representative section is shown, scale bar = 10μm. Blue (DAPI), DNA; red, β-gal (SF-1 neurons); green, PIP₃.

c) Quantification of PIP₃ immunoreactivity of SF-1 VMH neurons in SF-1^{LacZ} and d) SF-1^{LacZ:ΔIR} reporter mice after saline, or insulin stimulation for either 10 or 20 min. Values are means ± SEM of sections obtained from at least three mice per stimulation and genotype. We counted in total 4400 neurons per genotype and quantification was performed as described in methods.

e) In situ hybridisation for IR-mRNA expression in SF-1^{LacZ} and SF-1^{LacZ:ΔIR} reporter mice (red). SF-1 positive cells were visualized by anti-β-galactosidase immunostaining (green) and nuclei were stained by DAPI-staining (blue). Representative sections are shown (scale bar = 10μm) and a quantification of VMH IR-mRNA expression in SF-1^{LacZ} and SF-1^{LacZ:ΔIR} mice normalized to that of SF-1^{LacZ} animals.

f) Western blot analysis of IR-β subunit and α-tubulin (loading control) in hypothalamus (HT), rest brain (RB), pituitary (Pit), liver, skeletal muscle (SM), pancreas (Panc), white (WAT) and brown (BAT) adipose tissue in control and SF-1^{ΔIR}-mice (n = 4 in each group).

Figure 2. Effects of insulin on electrical activity of VMH neurons.

- a) Representative recording of an identified insulin responsive SF-1-positive neuron in a hypothalamic slice from a SF-1^{GFP} mouse before and during addition of 200 nM insulin, followed by application of 200 μ M tolbutamide
- b) Representative recording of an identified SF-1-positive neuron from a SF-1^{GFP:ΔIR} mouse before and during addition of 200 nM insulin, followed by application of 200 μ M tolbutamide.
- c) Percentage of insulin-response SF-1 neurons from SF-1^{GFP} mice and SF-1^{GFP:ΔIR} mice.
- d) Membrane potential of identified SF-1 neurons in hypothalamic slices from SF-1^{GFP} mice before and during application of 200nM insulin, followed by addition of 200 μ M tolbutamide (n= 6 neurons per group). Firing frequency of identified SF-1 neurons in hypothalamic slices from SF-1^{GFP} mice before and during application of 200nM insulin, followed by addition of 200 μ M tolbutamide (n= 5 neurons per group).
- e) Membrane potential of identified SF-1 neurons from SF-1^{GFP:ΔIR} mice before and during application of 200nM insulin, followed by addition of 200 μ M tolbutamide (n= 12 neurons per group). Firing frequency of identified SF-1 neurons from SF-1^{GFP:ΔIR} mice before and during application of 200nM insulin, followed by addition of 200 μ M tolbutamide (n= 9 neurons per group).

Displayed values are means \pm S.E.M.; *, $p \leq 0.05$; **, $p \leq 0.01$.

Figure 3. Protection against diet-induced obesity in SF-1^{ΔIR}-mice.

- a) Average body weight of male control and SF-1^{ΔIR}-mice on high-fat diet (HFD) and male control mice on normal chow diet (NCD) (n>15 per genotype and diet).
- b) Epigonadal fat pad of male control and SF-1^{ΔIR}-mice on normal chow diet (NCD) or high-fat diet (HFD) at the age of 20 weeks (n>15 per genotype and diet).
- c) Body fat content as measured by NMR of male control and SF-1^{ΔIR}-mice on normal chow diet (NCD) or high-fat diet (HFD) at the age of 20 weeks (n>15 per genotype and diet).

- d) Serum leptin levels of male control and SF-1^{ΔIR}-mice on normal chow diet (NCD) or high-fat diet (HFD) at the age of 8 and 20 weeks (n>15 per genotype and diet).
- e) Quantification of mean adipocyte surface in epigonadal adipose tissue of male control and SF-1^{ΔIR}-mice on NCD or HFD at the age of 20 weeks (n>3 per group and diet).
- f) Representative H&E stain of epigonadal adipose tissue of male control and SF-1^{ΔIR}-mice on HFD at the age of 20 weeks. Scale bar = 100 μm.

Displayed values are means ± S.E.M.; *, p ≤ 0.05; **, p ≤ 0.01; ***, p ≤ 0.001. § p ≤ 0.01

Figure 4. Increased leptin sensitivity in young SF-1^{ΔIR}-mice.

- a) Daily food intake of male control and SF-1^{ΔIR}-mice on HFD at the age of 6 to 7 weeks (n> 16 per group)
- b) Oxygen consumption of male control and SF-1^{ΔIR}-mice on HFD at the age of 6 to 7 weeks (n>16 per group)
- c) Daily food intake of male control and SF-1^{ΔIR}-mice on HFD at the age of 12 to 13 weeks (n>14 per group).
- d) Oxygen consumption of male control and SF-1^{ΔIR}-mice on HFD at the age of 13 to 14 weeks (n>14 per group).
- e) Leptin sensitivity of 7- to 8-week-old male control and SF-1^{ΔIR}-mice on HFD, 4 and 8 hours after overnight fasting and i.c.v. injection of either ACSF or 5μg leptin. *, p ≤ 0.05 in an unpaired, one-tailed student's t-test.

Displayed values are means ± S.E.M.; *, p ≤ 0.05.

Figure 5. Protection against diet-induced insulin resistance in SF-1^{ΔIR}-mice.

- a) Random fed blood glucose levels male control and SF-1^{ΔIR}-mice on NCD and HFD at the age of 8 and 20 weeks (n>14 per group).
- b) Serum insulin levels in male control and SF-1^{ΔIR}-mice on NCD and HFD at the age of 8 and 20 weeks (n>14 per group).
- c) Intraperitoneal insulin tolerance test in male control and SF-1^{ΔIR}-mice on HFD at the age of 14 weeks (n>18 per group).
- d)) Intraperitoneal glucose tolerance test in male control and SF-1^{ΔIR}-mice on HFD at the age of 15 weeks (n>18 per group).

Displayed values are means ± S.E.M.; *, p ≤ 0.05; **, p ≤ 0.01.

Figure 6. Enhanced PI3kinase activation in the VMH promotes hyperphagia and weight gain.

- a) Double immunohistochemistry for lacZ and PIP₃ of ventromedial hypothalamic neurons of HFD-exposed SF-1^{LacZ} and SF-1^{LacZ:ΔIR} reporter mice was performed after an overnight fast. Shown is the percentage of SF-1 VMH neurons with low, moderate and high PIP₃ immunoreactivity (see methods for quantification). (n=3 animals per group).
- b) Double immunohistochemistry for lacZ and PIP₃ of ventromedial hypothalamic neurons of NCD-exposed SF-1^{LacZ} and SF-1^{LacZ:ΔPTEN} reporter mice was performed in overnight-fasted animals. Shown is the quantification of neurons with low, moderate and high PIP₃ levels (as displayed in Figure 1b). (n= 3; 2).
- c) Average body weight of male control and SF-1^{ΔPTEN}-mice on normal chow diet (NCD) or high-fat diet (HFD) (n>12 per genotype and diet), and SF-1^{ΔIR:ΔPTEN}-mice on high-fat diet (HFD).
- d) Daily food intake of male control and SF-1^{ΔPTEN} mice on NCD at the age of 10 weeks (n=8 per group).
- e) Epigonadal fat pad mass of male control and SF-1^{ΔIR:ΔPTEN}-mice on high-fat diet (HFD) at the age of 20 weeks (n>13 per genotype).

f) Quantification of mean adipocyte surface in epigonadal adipose tissue of male control and SF-1^{ΔIR:ΔPTEN}-mice on HFD at the age of 20 weeks (n>3 per group).

g) Body fat content as measured by NMR of male control and SF-1^{ΔIR:ΔPTEN}-mice on high-fat diet (HFD) at the age of 20 weeks (n>13 per genotype).

Displayed values are means ± S.E.M.; *, p ≤ 0.05; **, p ≤ 0.01.

Figure 7. Increased firing rate of POMC neurons of SF-1^{ΔIR}-mice compared to controls upon high-fat feeding.

a) Hypothalamic mRNA expression of pro-opiomelanocortin (POMC), agouti-related protein (AgRP), neuropeptide y (NPY) and cocaine-and-amphetamine-related transcript (CART) in control and SF-1^{ΔIR}-mice on HFD (n=6 per genotype).

b) Hypothalamic mRNA expression of steroidogenic factor (SF)-1 and brain-derived neurotrophic factor (BDNF) in control and SF-1^{ΔIR}-mice on HFD (n=6 per genotype).

c) Representative recording traces of POMC neurons in POMC^{GFP} and POMC^{GFP};SF-1^{ΔIR}-mice on HFD.

d) Mean firing frequency of POMC neurons in POMC^{GFP} and POMC^{GFP};SF-1^{ΔIR}-mice on HFD (n=4-5 animals per genotype; n=13-14 neurons per genotype). *, p ≤ 0.05 in an unpaired, one-tailed Student's t-test.

e) Proportion of silent POMC neurons in POMC^{GFP} and POMC^{GFP};SF-1^{ΔIR}-mice on HFD (n=4-5 animals per genotype; n=13-14 neurons per genotype).

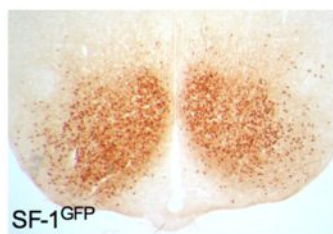
Displayed values are means ± S.E.M.; *, p ≤ 0.05.

Table 1

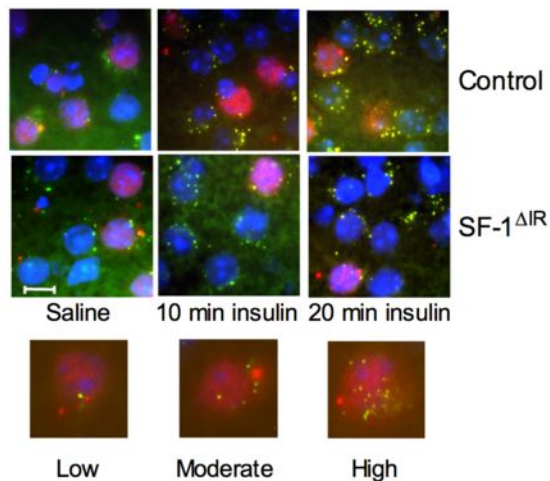
	Whole-Cell Capacitance (pF)	Firing Rate (Hz)	Membrane Potential (mV)	Input Resistance (GΩ)
SF-1^{GFP}	12.5 ± 1.0 (n=14)	3.5 ± 0.5 (n=13)	-46.8 ± 1.0 (n=14)	1.24 ± 0.12 (n=14)
SF-1^{GFP:ΔIR}	16.5 ± 1.8 (n=12)	2.9 ± 0.5 (n=9)	-48.5 ± 1.7 (n=12)	1.51 ± 0.24 (n=11)

Table 1. Electrophysiological parameters of SF-1 neurons in SF-1^{GFP} and SF-1^{GFP:ΔIR} mice. Depicted are electrophysiological parameters of SF-1 neurons in SF-1^{GFP} and SF-1^{GFP:ΔIR} mice. Values are given as mean ± SEM. The parameters were not significantly different between the two genotypes.

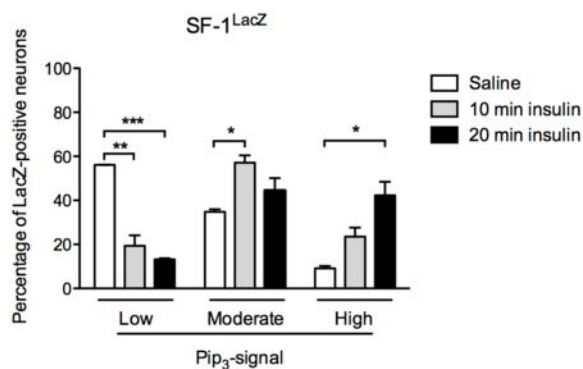
a



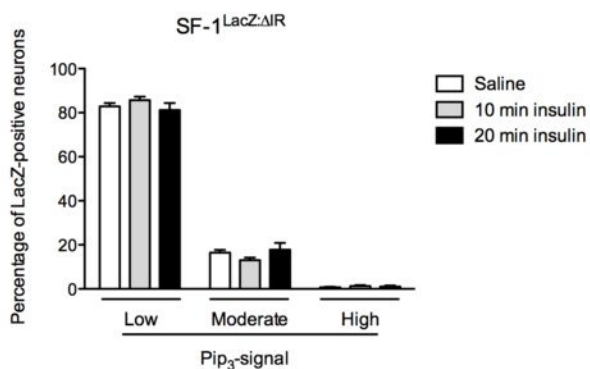
b



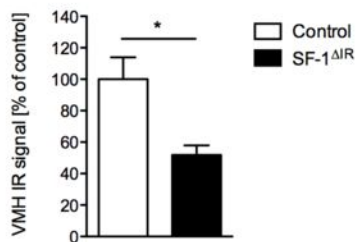
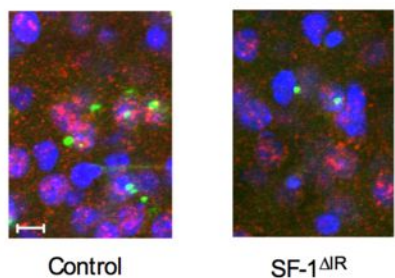
c



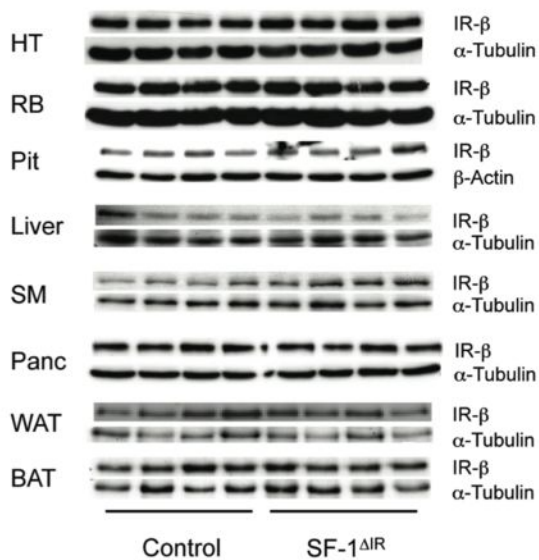
d



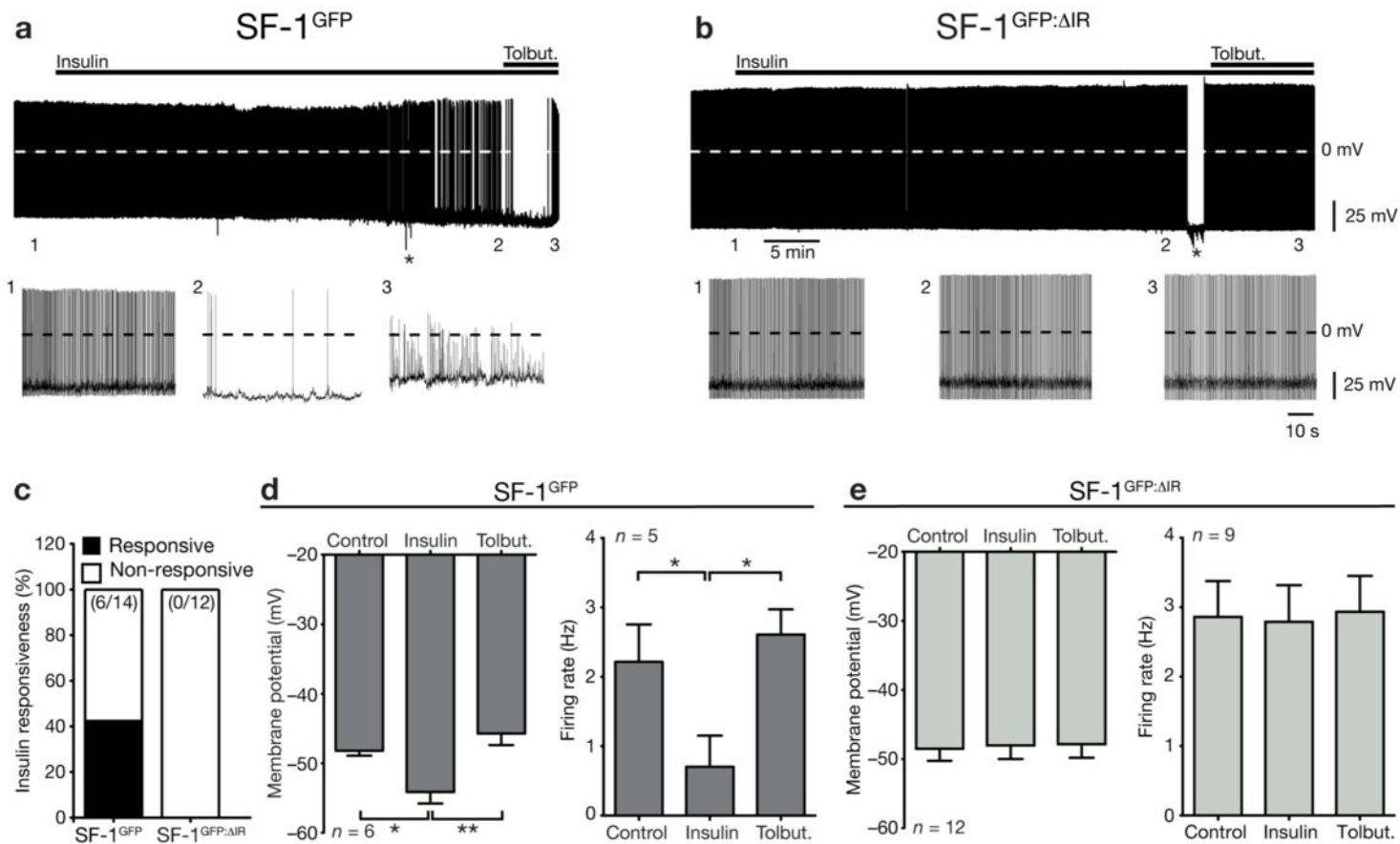
e



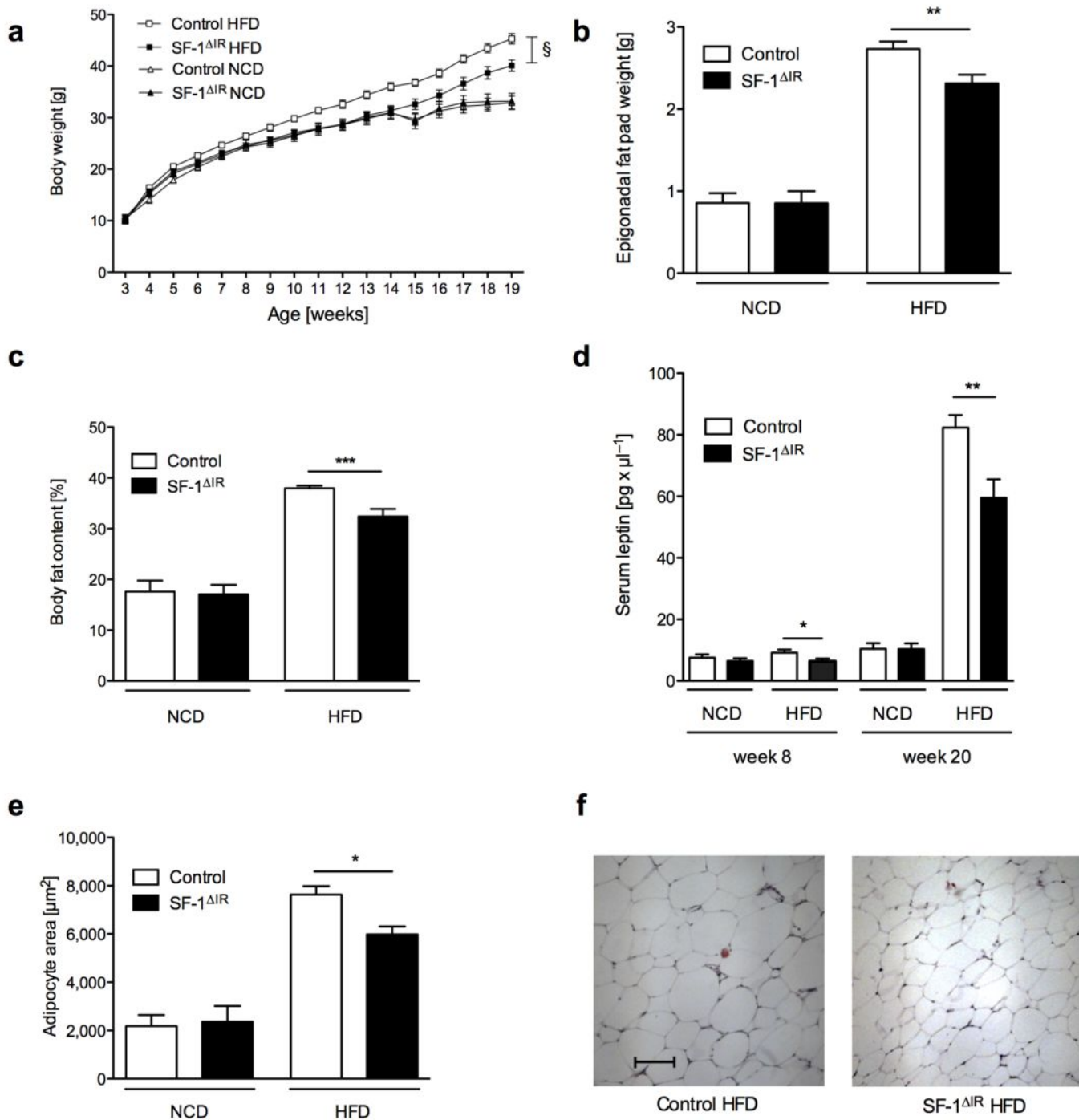
f



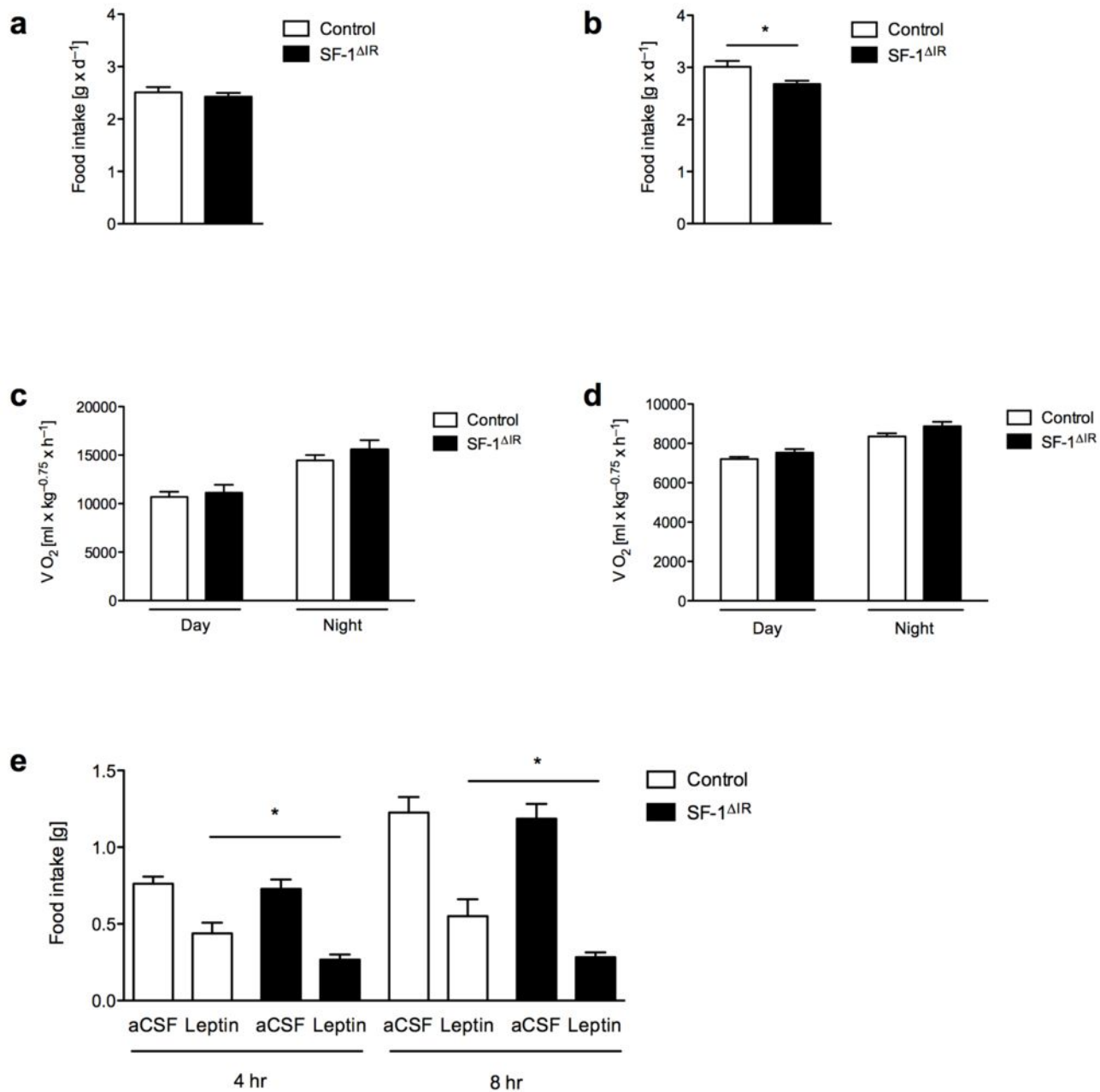
Klöckener et al. Figure 2



Klöckener et al. Figure 3

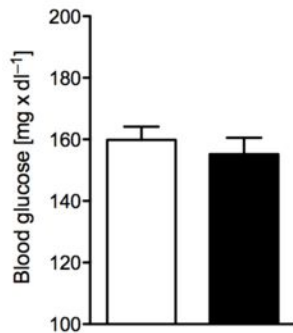


Klökener et al. Figure 4

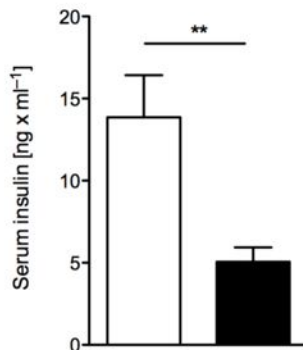


Klöckener et al. Figure 5

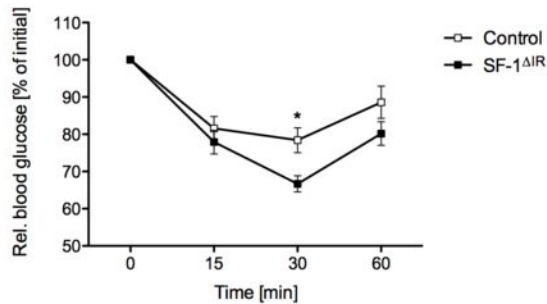
a



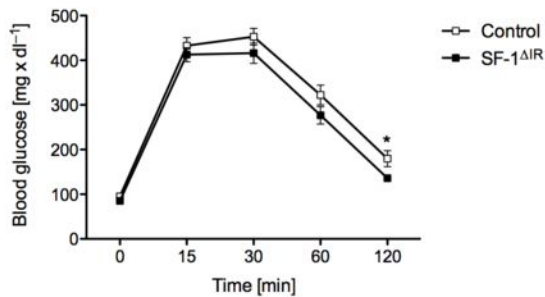
b

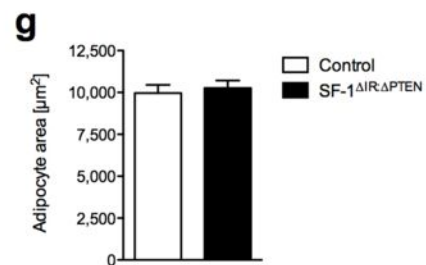
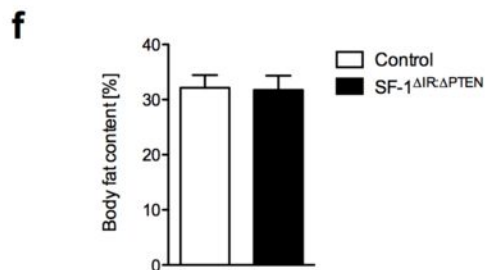
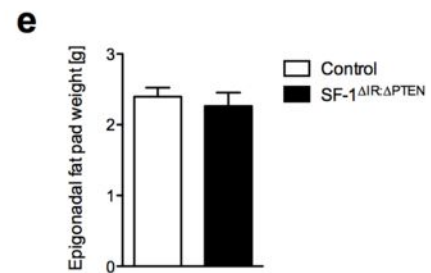
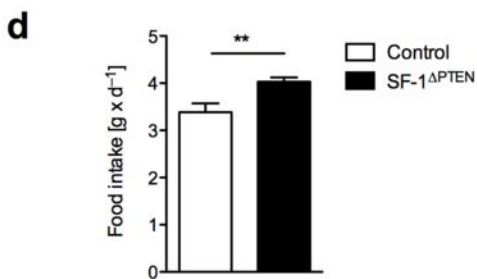
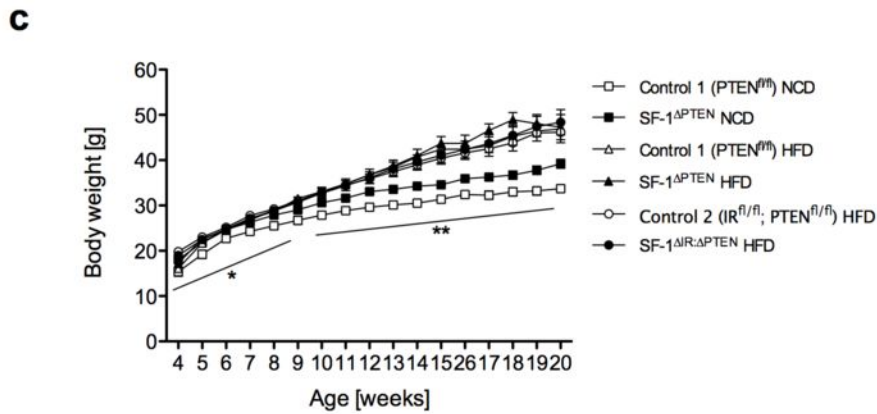
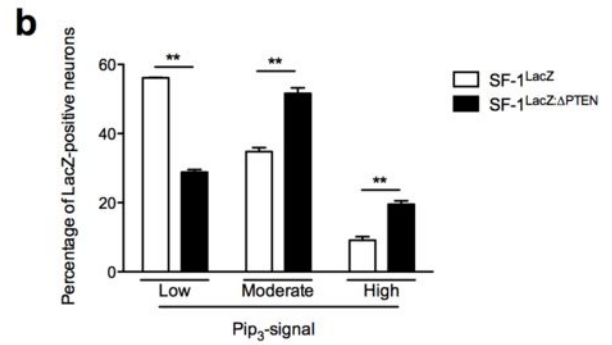
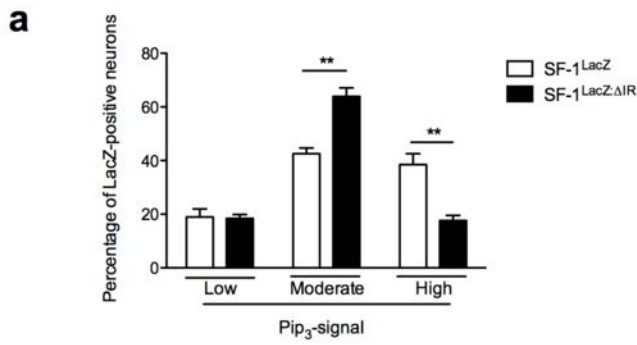


c



d





Klökener et al. Figure 7

